Penerbit Akademia Baru

Journal of Advanced Research in Fluid Mechanics and Thermal Sciences

Journal homepage: www.akademiabaru.com/arfmts.html
ISSN: 2289-7879

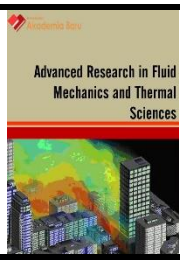


# Comparative Experimental and Numerical Investigations on the Characteristics of Air/Water Slug Flow in Horizontal Pipes

Open Access

Hussain H. Al-Kayiem[1,*], Zahid I. Al-Hashimy[2], Rune W. Time[3], Zena K. Kadhim[4]

[1] Mechanical Engineering Department, Universiti Teknologi PETRONAS, 32610 Bandar Seri Iskandar, Perak, Malaysia
[2] Iraq Ministry of Oil, OPDC, Baghdad, Iraq
[3] University of Stavanger, N 4036 Stavanger, Norway
[4] Mechanical Engineering Department, Wasit University, Wasit, Iraq

**ARTICLE INFO**

***Article history:***
Received 16 September 2019
Received in revised form 5 November 2019
Accepted 17 November 2019
Available online 4 February 2020

**ABSTRACT**

Prediction of flow conditions at which slugs are formed and characterisation of slugging are critical technological problems that are not fully resolved yet. This study experimentally and numerically investigated the characteristics of air/water slug flow by documenting the effect of different air and water superficial velocities on water slug length and frequency. The investigations focused on slug frequency, slug length, slug initiation in the pipe and liquid holdup. Experiments were conducted using a 0.074-m-diameter horizontal acrylic pipe with an 8.0-m length. A high-speed video camera was used to obtain the image sequence of the slug flow covering ranges of 0.7–3.5 and 0.65–1.23 m/s air and water superficial velocities, respectively. Numerical simulations were performed using a 3D implicit unsteady volume of fluid model with STAR-CCM+ code. The comparison of simulation experiments exhibited a reasonable agreement within a 10.4% relative error. The time traces of water holdup indicated that slugs are formed as a result of local instability at the wave crest rather than due to the instability of the entire wave. Mean water slug lengths ranged within 3.5–15 $D_{pipe}$. By increasing the air superficial velocity by 50% and fixing the water superficial velocity, the slug frequency decreased by 0.25 Hz. When the air superficial velocity was fixed and the water superficial velocity increased by 50%, the frequency rate was increased by 1.88 Hz.

***Keywords:***
Slug flow; slug frequency; slug length; slug initiation; VOF



## 1. Introduction

Slug flow is a prevalent multiphase flow regime realised in pipe flow, which imposes a major challenge to the flow assurance in the oil and gas industry due to the associated instability. The oil and gas industry encounters slug flow in production and transportation processes. Sharma *et al.,* [1] and Godhavn *et al.,* [2] classified slug flow into three different types based on its formation mechanism: hydrodynamic, operationally induced and terrain-generated slugs.

* *Corresponding author.*
*E-mail address: hussain_kayiem@utp.edu.my (Hussain H. Al-Kayiem)*

Issa and Kempf [3] elucidated that slug flow is initiated from stratified flow by reason of two broad hydrodynamic mechanisms. Firstly, the natural growth of hydrodynamic wave instabilities generated on the gas-liquid interface. Secondly, the accumulation of liquid caused by sudden pressure and gravitational force imbalance is due to undulation in the pipeline geometry. From another point of view, Sanchis [4] described the growth of hydrodynamic wave instabilities based on the classical Kelvin Helmholtz (KH) instability mechanism which indicates that when the difference between the gas and liquid flow rates is high enough resulting in an unstable hydrodynamic behaviour. On other hand, Sharma *et al.,* [5] highlighted the complexity of quantify and characterize the slug flow due to the large number of variables associated with the slug flow phenomena. As a result of occasional and intermittent character of the slug flow, the slug variables tend to be differing over time, and along the pipe flow. Slug length, slug frequency, water volume fraction distribution, slug velocity, momentum and energy transfer around the interface would be the most crucial variables to define the slug flow.

With regards to the slug length, numerous investigators have an interest in determining the actual liquid slug length or the slug body length. The mean slug body length, measured by Dukler and Hubbard [6], was found to be about 12D-30D regarding air-water flow in 38.1 mm pipe diameter. Nicholson *et al.,* [7], as well as Gregory *et al.,* [8], concealed a fixed dimensionless slug length of almost 30D for air-light oil flows in 0.0254 m (1 inch) and 0.0512 m (2 inch) pipes diameters. An empirical correlation generated from experimental data acquired from 0.0254 m pipe diameters was suggested by Scott *et al.,* [9]. The correlation shows that the average slug length, anywhere in the slug flow, is within the order of 30D. Alternatively, Nydal *et al.,* [10] carried out experimental measurement pertaining air-water flow and reported 15D-20D and 12D-16D for pipes diameters of 0.0512 m and 0.090 m (2 and 3.5 inches), respectively. Most of these reports concluded that slug length being sensitive to gas and liquid flow rate and relies primarily on the pipe diameter.

Slug frequency is described as the overall number of slugs appears at a specific interval of time, which is captured using a fixed observer. This particular parameter, in the slug flow studies, has not explored extensively because of the higher complexity. However, Fan *et al.,* [11] studied the transition from a stratified to a slugging pattern for the air–water flow in a 0.09 m pipeline. The slug frequency was measured with a piezoelectric pressure transducer mounted flush with the wall close to the pipe exit. It was found that for a given water superficial velocity, $U_{SW}$, the minimum slug frequency was found at approximately air superficial velocity $U_{SG}$ = 4 m/s, for all water superficial velocity range, 0.5 to 1.2 m/s. Measurements results of the slug frequency by Woods and Hanratty [12] are presented in terms of the formation of the slugs for an air–water flow in a 0.0763-m-diameter pipe for 1.2 > $U_{SW}$ > 0.4 m/s. They are similar to those reported by Fan and Hanratty [11], in which the frequency was proportional to $U_{SW}$ and the minimum was observed at around $U_{SG}$ = 4.0 m/s. How slug frequency effecting the stresses of the piping system is analyzed and reported by Mohmmed *et al.,* [13] through series of experimental tests to address the effect of the slug frequency on the stresses of structural pipes. They have proved that the piping structures are subjected to considerable fatigue due to the existence of slug liquid/gas flow.

Statistical techniques have been adopted by some groups of researchers as analysis and presentation tools of slug parameters. Carneiro *et al.,* [14] have examined, experimentally and numerically, the slug frequency and slug length in transparent horizontal test section of 10.0 meters long and 24.00 mm internal diameter using air and water as the working fluids. The flow was numerically determined based on the one-dimensional Two-Fluid Model. Differences between measured and predicted values were 10% and 20% for frequency and slug length, respectively. Al-Kayiem *et al.,* [15] have examined the slug flow experimentally using air/water two phase flow in 0.074-m-diameter horizontal pipe. The superficial velocities have been varied within ranges of 0.7 to

3.84 m/s for air and 0.7 to 1.33 m/s for water. The experimental data have been collected using non-intrusive optical based technique. They presented their results in statistical format for the translational slug velocity and slug body length. They concluded that for fixed water velocity, the slug length increased with increasing the air velocity while the slug frequency decreased. Whilst for fixed air velocity, the slug length decreased with increasing in the water velocity whiles the slug frequency increased.

An experimental and numerical study of flow pattern and void fraction using water–air was implemented by López *et al.,* [16]. The results were obtained experimentally inside short horizontal pipe of 2-m-length and 14-mm-inner diameter, using High Speed Filming (HSF) analysis. STAR-CCM+ software version 10.02.012 (CD-ADAPCO) was used to perform the simulation of the two phases traveling inside the pipe. CFD approach in STAR-CCM+ software was also used by Pineda-Péreza *et al.,* [17] to simulate slug flow of air with high viscosity liquid in 50.8-mm-diameter horizontal pipe by Volume of Fluid (VOF) method. They presented the results in terms of velocity profile and they concluded that the velocity fields showed the regions where the gas bubbles are entrained in the slug body. They haven't presented data on the slug initiation, slug frequency and /or the slug body length.

Previous studies on slug flow characterisation have utilised pipes with a small diameter, mostly less than 60 mm. Most of these studies are experimental in nature because the repeatability of the experiments with changes/modifications in the experimental setup is costly and time consuming, which is why the cases are limited to narrow boundary conditions. In addition, the associated data of slug flow characteristic, slug initiation, slug length and slug frequency, which are generated from validated simulations through experimental referencing, are limited. The field of slug flow requires sophisticated data to enhance the understanding and analysis of the slug phenomena. The present work is motivated by a hands-on industrial problem associated with the piping system in an offshore platform. The slug flow imposes a large amount of cyclic momentum and pressure forces, which are not accounted in the 1D design software. Understanding the slug flow and prediction of pressure forces, stress generation and vibration associated with the presence of slug flow is essential in extending the prediction and understanding of the parameters that were not captured by the OLGA software because a large amount of experimental investigation is impractical. Hence, additional numerical data from validated numerical simulations are necessary to develop reliable correlations that will allow mathematical modelling and enhance the capabilities of the design software in the oil and gas industry for designing the piping systems and processing facilities.

The aim of this study is to implement and compare a computational fluid dynamics (CFD) simulation with the experimental results in terms of slug initiation, slug length and slug frequency of the air/water flow in horizontal pipe. The air and water superficial velocities were varied, and the slug parameters were experimentally measured and numerically predicted. The measurements and simulation were conducted in a 0.074-m-diameter (3 in. standard) pipe, which is relatively large compared with the pipes used by previous works. The two phases were air and water with various ranges of superficial velocities.

## 2. Experimental Setup and Procedure

The experimental setup, equipped with a sophisticated measurement system, was designed and constructed in the fluid laboratories of the Mechanical Engineering Department at Universiti Teknologi PETRONAS. The facility comprises flow loop and monitoring/control structures for data acquisition. The major components of the facility include the test section, air and water supply systems, a two-phase mixer and a high-speed video system.

### 2.1 Experimental Flow Loop

Slug flow experiments were conducted using a mixture of air and water flowing in an 8-m-long pipe with an inner diameter of 0.074 m. Figure 1 shows the schematic of the experimental flow loop system.

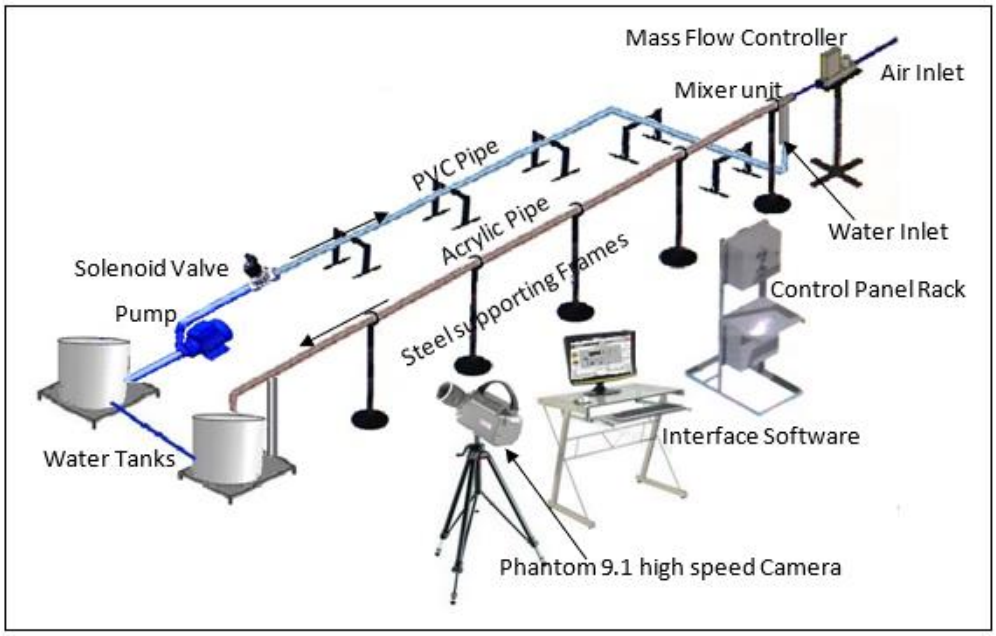


**Fig. 1.** Schematic of the experimental system

The flow line was placed at two levels. Water pump and the water supply pipe were placed at the lower level. The two-phase flow testing pipe was placed as the upper level. The lower pipe, which supplies water, was connected to a mixer at the inlet of the two-phase flow pipe. Air is supplied to the mixer from the main air compressor line in the fluid Lab, at maximum air flow rate of 42.5 $m^3$/min pressure up to of 0.85 MPa. The water feed pipe was made of PVC with 7 m length and 50.8 mm diameter installed on six supports anchored to the ground to prevent the literal moving and was connected to the mixer by flexible hose to avoid the vibration that may occur in the pipe generated from the pump. Such flexible connection was found to be necessary to avoid the vibration transfer from the water supply pipe to the test pipe, and also simplify the dismantling and assemble of the piping system. Water was stored in a 0.454 $m^3$ (100 UK gallon) capacity tank, which was used to feed the closed loop through the lower PVC water supply pipe. Another tank, with capacity of 0.363 $m^3$ (80 UK gallons) was used to accumulate the return water from the test section. The purpose of the 0.363 $m^3$ tank is to prevent the pump from the debris and air bubble.

The air and water phases are combined at the beginning of the pipeline in a tee mixer section with the water phase in the run, and the air phase entering from the top of the tee section through 0.02 m diameter flexible hose parallel to the main flow into the mixer as shown in Figure 2. The mixer is made of PCV with T-section shape has two inlets one outlet. All opens have 74.0 mm diameters. The mixture section was designed with an elongated plate, phase separation plate, in the middle to separate the air and water. The objective of this modification is to determine the void and water holdup at the inlet are 50%.

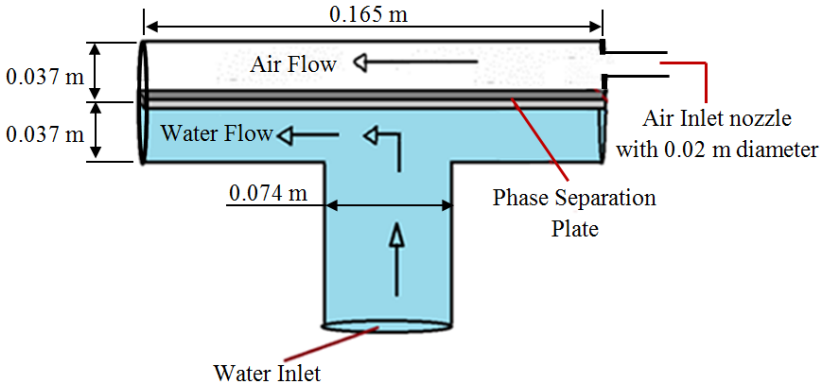


**Fig. 2.** Air/water mixer section at the inlet of the 8.0-m-long pipe

*2.2 Measurement Strategy*

Water was fed to the test loop using pump, type EBARA 3M 50-125/2.2, with maximum flow rate of 1.0 $m^3$/min and 19.0 m pressure head. Calibrated ultrasonic flow meter with accuracy of ±0.5% was utilized to measure the water flow rate. A solenoid valve was used to open/close the water supply loop. The air flow rate was controlled and measured by calibrated (Omega FMA-2600A) mass flow controller which measure air flow within the range from 0-2 $m^3$/min with accuracy of ±0.01%.

The test section was made of acrylic. Transparency of the acrylic pipe allows visual observations of the flow behaviour. It consists of four separate pipe section, each of 2.0 m length, connected by flanges that could be easily dismantled and re-assembled. The flanges were installed above a rigid steel support frames anchored to the ground to insure fixed support. The slug flow characteristics had been measured at a distance of 6.0 m from the inlet. This distance from inlet provides enough length for the slug growth and development.

In order to accomplish the desired water and air flow rates in the flow loop, a control/monitoring electromechanical assembly was designed and implemented comprising hardware and software parts. It was basically utilized LabVIEW tools and interface hardware. The electromechanical assembly was interfaced with the pump, for water flow control and monitor, and air mass flow controller, to control and monitor the air flow rate. Graphical User Interface (GUI) enabled selection and setting of the air and water flow rate through the PC.

A high speed video system was used to observe the characteristics of air-water slug flow. It consists of a Phantom 9.1 high speed video camera, connection cable and processor. The system was supplied with full control and image download software. A typical sequence snapshot recorded by the camera using a recording rate of 1000 frames per second, (fps), and reduced resolution up to 100,000 fps, the camera field of view is 960 (width) x 480 (height) pixels resolution and stored directly in the RAM of a personal computer and then transferred to a hard disk for permanent storage. A schematic diagram of the experimental setup and the camera configuration is shown in Figure 3.

High speed camera was used to capture the images of the moving slugs in the acrylic pipe. The snap shots were carried out at a location of about LP/D = 81 (~ 6 m downstream the inlet), where LP is the length of the pipe from the inlet to the measurement zone and D, is the pipe inner diameter. Each image frame was separated by a short period of time, depending upon the sample rate and the exposure of the camera, so that the displacement or deformation imposed by the fluid can be seen and recorded. A meter scale was installed in order to measure the length and the frequency of the moving slug. Further information on the developed technique for digitalization of the images could be found in Mohmmed *et al.,* [18] and more details, including the developed MATLAB code, are available in the PhD thesis of Mohmmed [19].

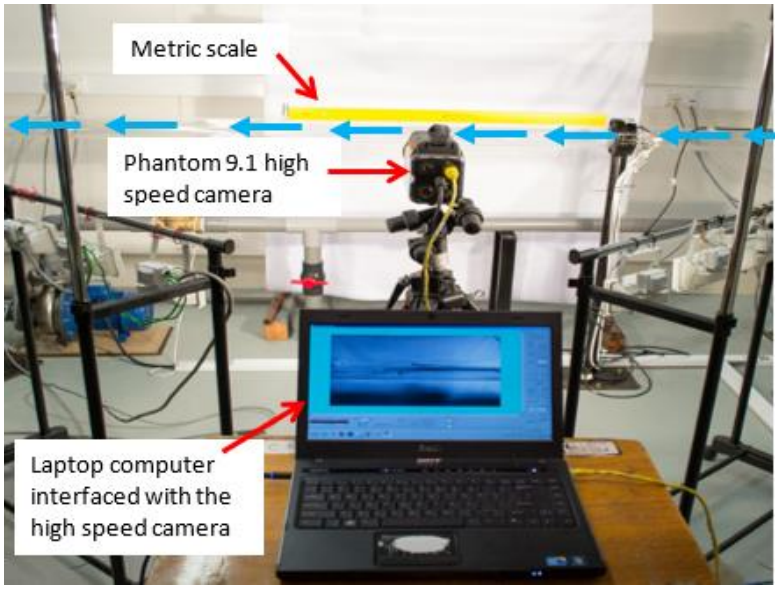


**Fig. 3.** Photograph of the high speed video camera arrangement

Uniform illumination over the whole test section is achieved by means of an illumination system composed of 10 fluorescent lamps as shown in Figure 4. The system was equipped with a diffusive white surface in front of the lamp for greater light uniformity.

The adopted procedure for the current experiment investigations was to select a fixed water superficial velocity and incrementally increasing the air superficial velocity up to the value in which the flow regime changes from slug flow to another flow regime, then increasing the water superficial velocity and repeating the previous steps.

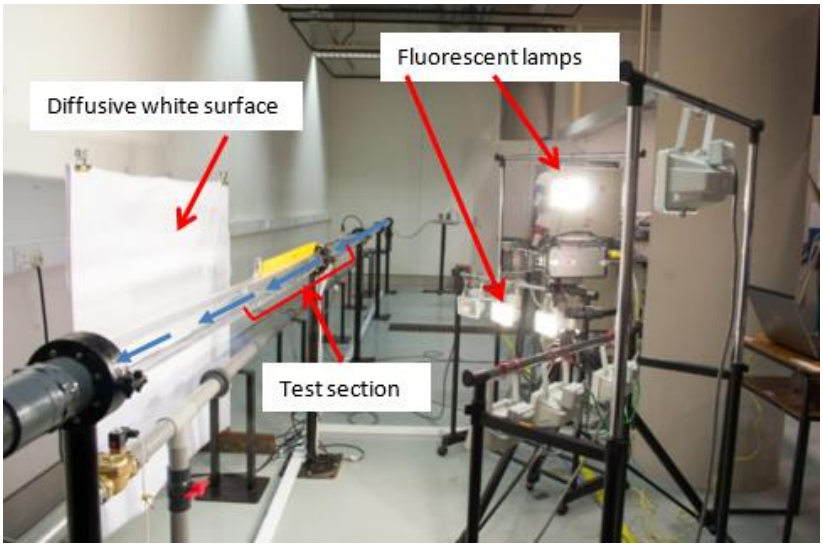


**Fig. 4.** The test pipe with lightening system

### *2.3 Uncertainty and Errors Analysis*

All the instruments used for the data acquisition have been calibrated prior to experiment commencement. The ultrasonic flow meter was calibrated by using Weighting Stop-Watch Devices using scaled container with volume of 0.454 $m^3$ and stop watching for this purpose. The process was repeated 5 times, with various flow rates. The measured verses calculated data showed mean error

of 0.26% mean error. Air mass flow meter was calibrated against Rotameter reading. The mean error was 3.3 %, with correlation coefficient $R^2$ of 0.99.

Following the normal procedure of measurement error of experimental variables outlined by IAEA 2008 [20], using the standard deviation method, the maximum uncertainty in the slug length measurement was estimated around ±0.02 mm.

## 3. Development of the Numerical Scheme

Pinilla *et al.,* [21] conducted a comparative study on the two-phase flow prediction of a 50.8-mm horizontal pipe, which covered four different regimes, including slug flow. They compared the results of CFD, OLGA software and 66 different empirical correlations. They concluded that the CFD simulation outperformed the other two methods in terms of the predicted flow patterns, pressure gradients and void fractions. The CFD simulation in the present study was performed using the software package STAR-CCM+ for adiabatic gas–liquid flow in a horizontal pipe. This software can effectively simulate complex flow phenomenon, such as the slug flow.

To compare the numerical and experimental results, the air/water phase couple was selected as the representative of the gas–liquid two-phase flow. Table 1 lists the properties.

**Table 1**
Physical properties of fluids

| Fluid | Density, $\rho$ [kg/m$^3$] | Viscosity, $\mu$ [Pa·s] | Surface tension, σ [N/m] |
|---|---|---|---|
| Water | 998.2 | $1.003 \times 10^{-3}$ | 0.07194 |
| Air | 1.225 | $1.855 \times 10^{-5}$ | - |

The experimental values of the void fraction and flow velocities of water and air at the inlet were adopted as the boundary conditions in the simulation procedure. The inlet velocity, outlet pressure and hydraulic smooth wall with non-slip boundary conditions were also utilised. The velocity–inlet boundary type was used. The most suitable boundary condition for the external faces of the incompressible water was the velocity–inlet, as recommended by Rashimi *et al.,* [22]. The average static pressure (P = 0 Pa) was applied to the downstream outlet boundary condition.

### *3.1 Model Development*

The geometrical values of the flow system used in the numerical analysis are like those of the test pipe used in the experiment (inner diameter = 0.074 m, length = 8 m). The pipe's axial axis is always aligned with the x-axis, and several cross sections can be placed along the pipe (Figure 5).

Initially, the upper 50% of the pipe was occupied by air and the lower 50% was occupied by water. The inlet phase distribution was fed to the pipe by using a sinusoidal function to agitate the free surface and accelerate the transition. Frank [23] expressed this function using the liquid level $y_1$ as

$$y_1 = y_o + A_1 \sin\left[2\pi \frac{U_{sw} \cdot t}{p_1}\right], \quad (1)$$

where $y_o = 0.0$, $A_1 = 0.25\ D$, $p_1 = 0.25\ L_p$ and $U_{sw}$ is the water superficial velocity.

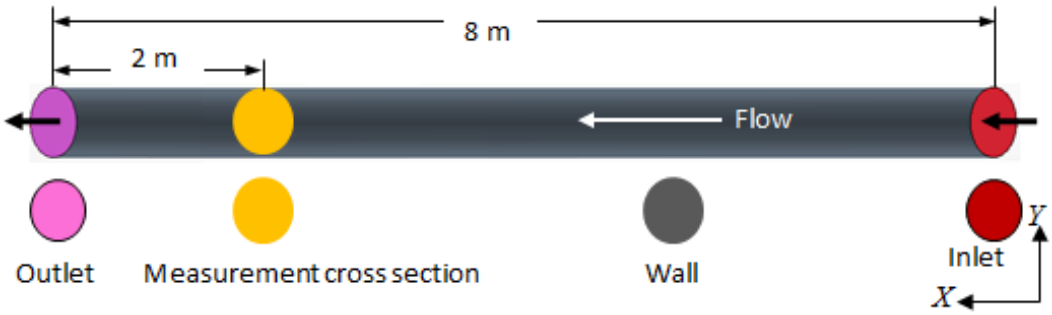


**Fig. 5.** Horizontal pipe geometry and measurement section in CFD

*3.2 Governing Equations*

When gas and water flow in a pipe, conditions exist for which the two phases are separated from each other by a surface interface. The gas–water flow can be observed in the horizontal pipeline and characterised by the structure of the interface, which can be smooth or wavy. The inlet and outlet faces consist of air and water inlet faces, wherein an in-between interface surface exists. The area of these faces depends on the water height $h_w$ or water holdup $\alpha_w$.

According to Al-Jassim [24], the geometrical relationship for the water phase holdup can be written as

$$\alpha_W = \left(\frac{1}{\pi}\right)\left\{\pi - cos^{-1}\left[2\frac{h_W}{D} - 1\right] + \left[2\frac{h_W}{D} - 1\right]\sqrt{1 - \left[2\frac{h_W}{D} - 1\right]^2}\right\}, \quad (2)$$

where the value of $h_w$ was already assumed at the beginning to calculate the other parameters, such as air and water areas, air and water perimeters and the interface length between the water and air. These parameters are necessary in meshing the computational domain.

The areas for the phases can be obtained as

$$A_k = \alpha_k \pi \frac{D^2}{4}, \quad (3)$$

where $k = G$ for the gas phase and $k = w$ for the water phase.

The general conservation equations for unsteady two-phase flow can be adopted as follows. Conservation of mass.

$$\frac{\partial \rho_m}{\partial t} + \frac{\partial}{\partial x_i}(\rho U_i) = 0, \quad (4)$$

where $i = x, y, z$ for velocity components $u$, $v$ and $w$, respectively, and

$\rho_m = \alpha_w \rho_w + \alpha_G \rho_G$.

The momentum equation was solved through the flow domain. The solution was dependent on the volume fraction of the two phases, and the fluid properties were used as mean values. Under such considerations, Lacovides *et al.,* [25] developed the momentum conservation equation for 3D unsteady air/water flow as follows:

$$\frac{\partial(\rho_m U_i)}{\partial t}+\frac{\partial}{\partial x_j}\left(\rho_m U_i U_j\right)=-\frac{\partial p}{\partial x_i}+\rho_m g_j+\frac{\partial}{\partial x_j}\left[\mu_m\left(\frac{\partial U_i}{\partial x_j}+\frac{\partial U_j}{\partial x_i}\right)-\rho_m\overline{u_i u_j}\right]+\bar{F}. \quad (5)$$

The shear stress transport (SST) model developed by Menter [26] utilises the *k-ω* model near the surface. An SST with *k-ω* turbulence modelling that can provide accurate formulations to solve all $y^+$ treatments using two equations was adopted. In addition, the model considers the transport of the turbulent shear stress, as well as provides the accurate predictions of flow separation due to adverse pressure gradients. For these reasons and the relatively high efficiency of numerical solutions, the two-equation SST *k-ω* model is widely adopted for the numerical simulation incorporated with high turbulence, as recommended by Yang *et al.,* [27]. The SST *k-ω* model was also adopted by Pineda-Péreza et al., 2018 in their CFD simulation of slug flow in a 50.8-mm-diameter horizontal pipe. The equations of the model involve two transport equations: one for the kinetic energy *k*, which determines the turbulence energy, and another is for the dissipation rate *ω*, which determines the turbulence scale. Eq. (6) and (7), which explain the SST *k-ω* model, are reported in detail by Wilcox [28].

Turbulent kinetic energy,

$$\frac{\partial(\rho k)}{\rho t}+\frac{\partial(\rho U_j k)}{\partial x_j}=P-\beta^*\rho k\omega+\frac{\partial}{\partial x_j}\left[(\mu+\sigma_k\mu_t)\frac{\partial k}{\partial x_j}\right] \quad (6)$$

Specific dissipation Rate,

$$\frac{\partial(\rho\omega)}{\partial t}+\frac{\partial(\rho U_j\omega)}{\partial x_j}=\frac{\gamma}{\nu_t}P-\beta\rho\omega^2+\frac{\partial}{\partial x_j}\left[(\mu+\sigma_\omega\mu_t)\frac{\partial\omega}{\partial x_j}\right]+2(1-F_1)\frac{\rho\sigma_{\omega 2}}{\omega}.\frac{\partial k}{\partial x_j}.\frac{\partial\omega}{\partial x_j} \quad (7)$$

where *ρ* is the density of fluid, k and ω are the turbulent kinetic energy and its dissipation frequency, respectively and *P* is the production of turbulent kinetic energy. $\nu_t=\mu_t/\rho$ is the turbulent kinematic viscosity, $\mu$ is the molecular dynamic viscosity.

### *3.3 Mesh Generation and Independency Check*

The computational model established using 3D discretisation was unsteady and implicit, which suits any type of multiphase mixture flow. The multiphase interaction option was used to identify the phase's interactions. The volume of fluid (VOF) approach was adopted to solve the interface between the phases using numerical grids that track the volume fraction of each phase at each flow field volume. Based on the law of the wall and the terminology of the dimensionless distance perpendicular to the wall, denoted by $y^+$, this approach provides acceptable results even when $y^+$ is between 1 and 30. The gravity effect was accounted (gravitational acceleration = 9.81 m/s$^2$). The mesh was developed using the directed mesh technique in the STAR-CCM+ software. The suitability of this technique for simulating a two-phase flow in a horizontal pipe with acceptable accuracy was confirmed by Pineda-Péreza *et al.,* [17], Mohmmed [19] and Al-Hashimy *et al.,* [29]. To identify the minimum mesh density that will make the solution independent of the mesh resolution, a mesh sensitivity analysis was performed using five different meshes.

One interesting aspect of the time trace in characterising the slug two-phase flow is the water holdup fluctuation. The slug frequency was experimentally obtained based on the time variant water holdup at various flow conditions. The simulation for one case study was conducted using the

following experimental inlet flow conditions: $U_{SG}$ = 3.141 m/s with 50% void fraction and $U_{SW}$ = 1.0 m/s with 50% holdup. For the first slug, the water reached the measurement section ($L_P$ at 81 D from the inlet) within slightly less than 3 s. Figure 6 shows the plots of the time history of the water holdup for the five tested meshes under the abovementioned conditions.

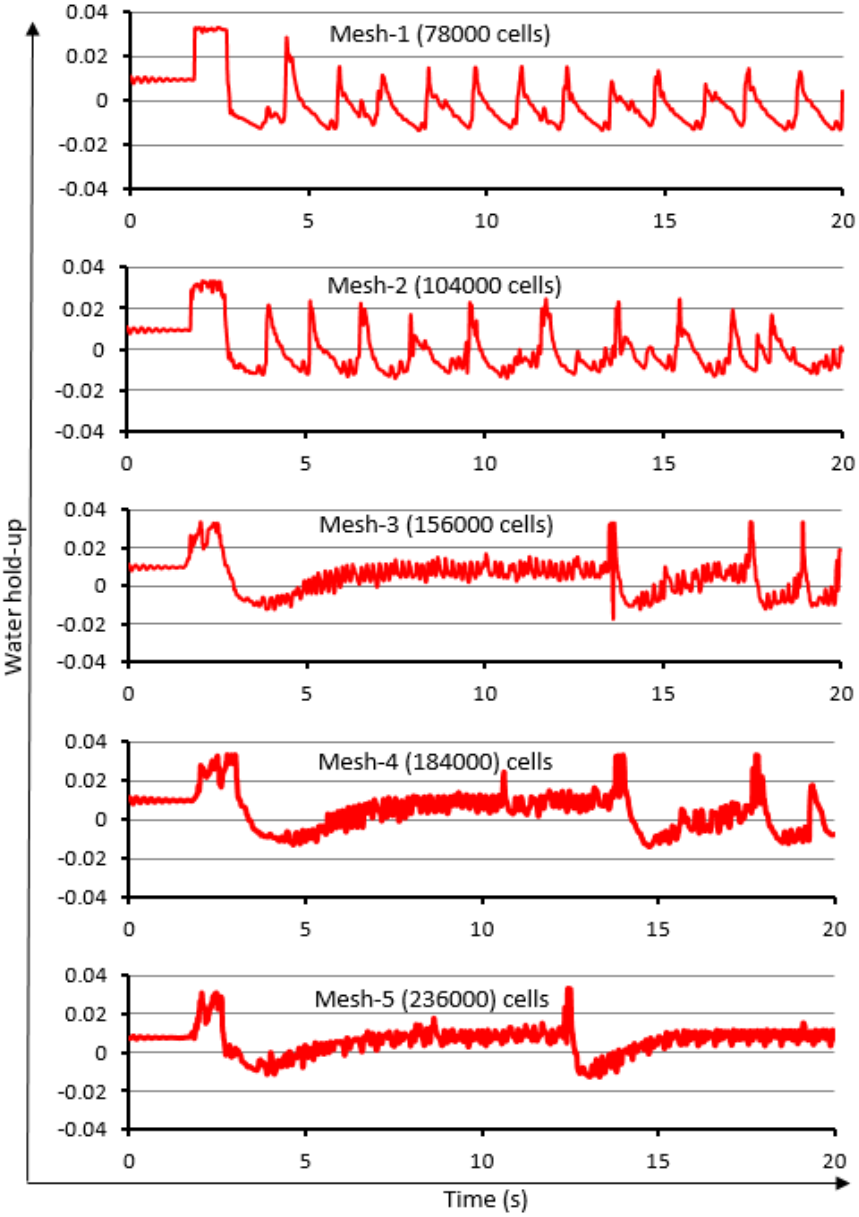


**Fig. 6.** Effect of grid size on the time traces of water holdup results at $L_P$ = 81 $D$ ($U_{SG}$ = 3.141 m/s, $U_{SW}$ = 1.0 m/s)

The comparison of the mesh sensitivity results indicates that Mesh-1 could simulate the slug flow pattern once. This high liquid, which looks up to the upper surface of the pipe, might not be a completed slug, but possibly a spurious wave. Whatever the case is, the mesh size in Cases 1 and 2 did not capture the repeatability of the slug. Hence, the numbers of cells increased. The case with Mesh-3, wherein the cell number is set to 156000, simulated the repeatability of the slug more than once, which is more acceptable than the experimental data in terms of slug frequency. Increasing the number of cells from Mesh-4 to Mesh-5 almost predicted the water slug with repeatability and did not influence the result of water slug frequency.

A further increase in the number of cells was not useful because of the corresponding increases in the required memory and computational time, consequently requiring a high computer specification in terms of RAM and processor. By contrast, many grid cells were considered disadvantageous. Hence, Mesh-3 (156000 cells) was used as the optimal number of cells in the simulation. Table 2 presents the mesh profiles tested in the current CFD simulation.

**Table 2**
Analysis of the mesh profiles for the selection of the appropriate mesh size

| Mesh name | Number of grid cells | Length of grid (mm) | Memory used (kb) | Criteria of goodness (repeatability of slugs) |
|---|---|---|---|---|
| Mesh-1 | 78000 | 26 | 48,663 | One slug and the others mostly wavy |
| Mesh-2 | 104000 | 20 | 62,649 | One slug and the others mostly wavy |
| Mesh-3 | 156000 | 13 | 117,642 | Repeated slugs |
| Mesh-4 | 184000 | 11 | 118,335 | Repeated slugs |
| Mesh-5 | 236000 | 8.8 | 153,756 | Repeated slugs |

### *3.4 Simulation Procedure*

An implicit method spread over iterations through time steps was used to calculate the variables based on the known and unknown values at the cells of the current time step n and the forward time step n+1. This method is computationally intensive, but it allows large time steps. As a result, all cells are coupled to each other and stabilised due to the independency of the time step. In this study, the implicit integration is applied to achieve fast convergence and avoid instability issues.

If the mesh is generated with fewer cells than the time step, numerical smearing might occur, which will lead to instability and even divergence in some cases [30]. To avoid this possibility, a match amongst fluid velocity $U_{air}$, cell size characterised by the cell length $\Delta x$ and time step $\Delta t$ was ensured by introducing the Courant–Friedrichs–Lewy (CFL) number (usually referred as the Courant number) to guarantee the convergence. CFL can be expressed as

$$\mathrm{CFL} = \frac{U_{air}\,\Delta t}{\Delta x} \tag{6}$$

The implicit solution method was selected over the explicit one to achieve a robust convergence. To achieve the fast convergence rate of the solution, Chica [31] suggested that CFL should not be larger than unity.

For all investigated cases in the simulation of air/water slug flow, $\Delta t$ = 0.003 s and $\Delta x$ = 0.013 m. The CFL was less than 1.0 to avoid any instability or possible numerical diffusion. In addition, the entire physical time t was set to 20 s, which is enough for the slug to be initiated, develop and travel to the end of the pipe, with repeated initiation of the next slug. Moreover, a second-order temporal discretisation pattern was used for the time domain solution. The high-resolution interface capturing scheme was used in this simulation to capture the interface between the two phases. Therefore, the surface tension force based on the continuum surface force was applied to the two phases.

## 4. Results and Discussion

Many slug characterisation parameters have been considered in the experimental and numerical procedures. Firstly, slug initiation, slug length and slug frequency were experimentally measured.

Then, the numerical procedure was validated by comparing the obtained mean slug length with the experimental results. Finally, the numerical results of the water slug development phenomena and the water holdup were addressed and analysed.

### *4.1 Analysis of Slug Initiation and Development*

#### *4.1.1 Experimental visualisation*

The designation of the slug flow pattern is largely based on an individual interpretation of the visual observation. This essential step was performed through the transparent pipe section of the rig using a high-speed video system, as well as the naked eye.

The visualisation of the flow development (Figure 7) demonstrated that slug formation is a three-stage process. Initially, the flow exhibited a stratified pattern, wherein the air was at the top and the water was at the bottom (Figure 7(a)). As the air passed over a water wave, a pressure drops occurred, followed by pressure recovery, thereby creating an upward directed force within the water wave (Figure 7(b)). The flow was a slug flow under the conditions that the upward force is enough to raise the wave to the top of the pipe. Figure 7(c) shows that once the water wave reached the top of the pipe, a familiar slug shape with a front and rear was formed. The water slug was pushed by the air and thus travelled with a larger velocity than the water layer at the bottom of the pipe.

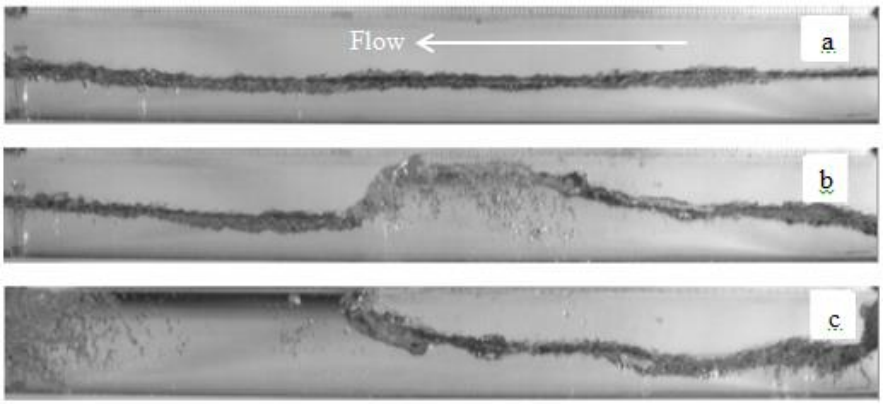


**Fig. 7.** Slug flow visualisations and developments for $U_{SG}$ = 2.094 m/s and $U_{SW}$ = 0.93 m/s: (a) stratified flow; (b) wavy flow; (c) slug flow

The effects of air and water inlet velocities on the slug initiation position were experimentally examined. Figure 8 presents the results. The slug initiation is strongly dependent on the water and air superficial velocities. At a fixed air superficial velocity, when the water superficial velocity increased, the slug initiation position would be transferred farther from the inlet. Conversely, at a fixed water superficial velocity, when the air superficial velocity increased, the slug initiation position would be transferred to a close distance from the inlet. The minimum initiation position from the entire investigated tests was 40 D.

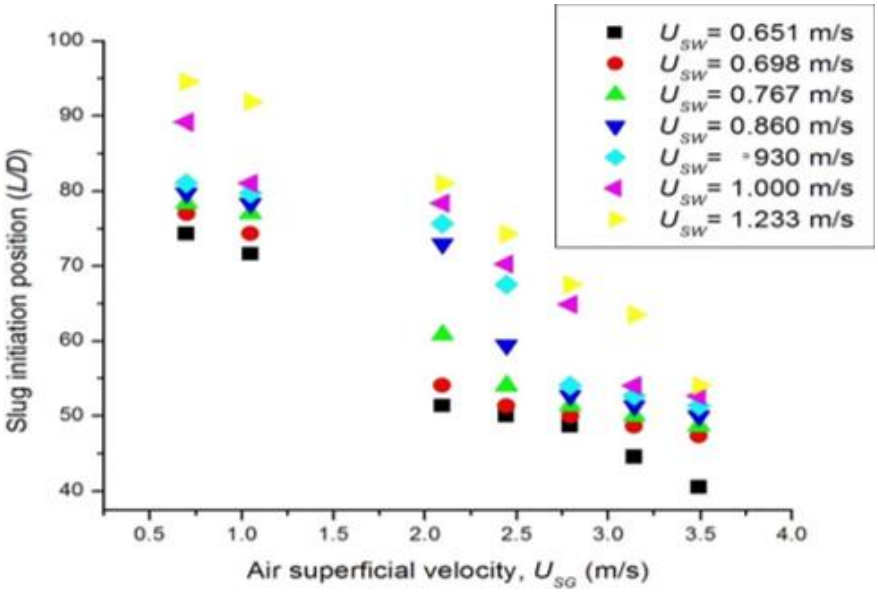


**Fig. 8.** Slug initiation positions for different air and water superficial velocities

### *4.1.2 Numerical visualisation*

Figure 9 shows the simulation results of Case 3 in terms of the void fraction of the air/water slug flow along the horizontal pipe. The distribution contours of the void fraction contours of water and air are quite evident.

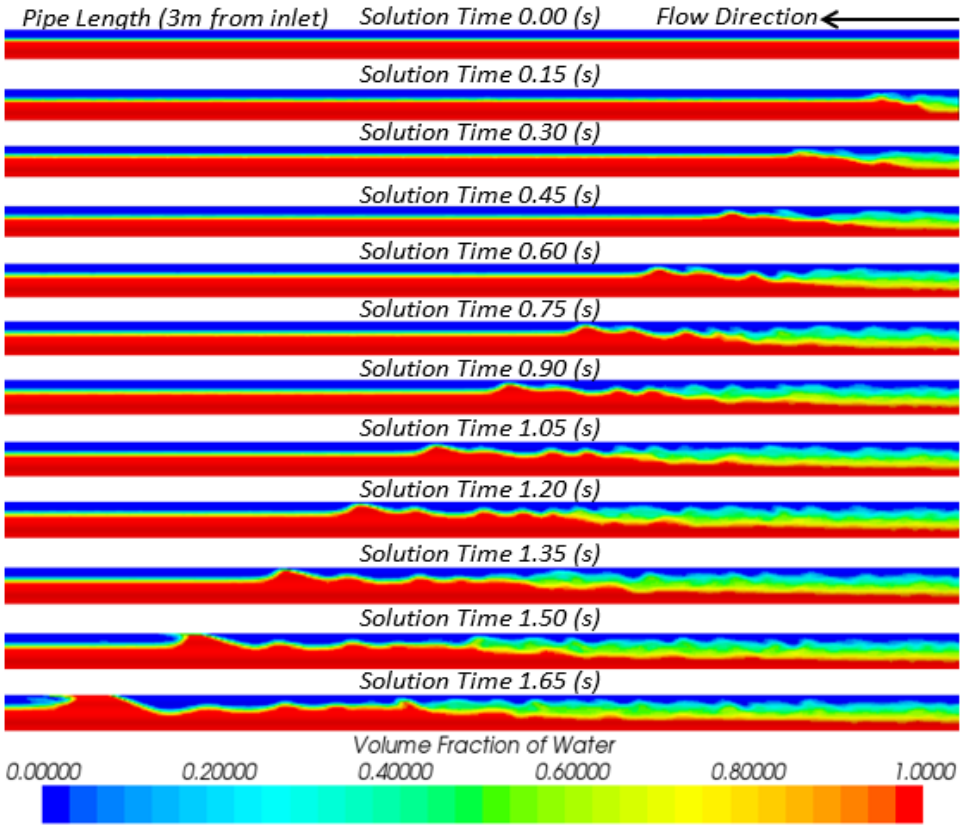


**Fig. 9.** Contours of the air/water slug flow formation under simulation Case 3 ($U_{SG}$ = 2.443 m/s and $U_{SW}$ = 1.0 m/s)

The red colour in Figure 9 is the water phase, whereas the dark blue colour is the air phase. The zone between the phases represents the interface surface. A sequence of instantaneous stages of the water slug formation process was presented. The stages were 0.15 s apart from each other. The process commenced from a state where t = 0 s (i.e. the flow along the pipe was stratified).

### *4.1.3 Water holdup analysis*

The simulation implied that the analysis of the water holdup is an interesting and important phenomenon in the slug flow. To follow the slug development, a set of time traces of the water holdup was captured at particular locations (Figure 10). The first cross-sectional area located at 54 D from the inlet showed a series of incipient slugs, which were initially characterised by slow growth. However, the slug started to build up rapidly, and the wave bridged the entire section of the pipe at 67.6 D. In conclusion, the slugs were formed as a result of the local instability at the wave crest rather than due to instability of the entire wave. This result confirms the conclusions of Kordyban 1985. The wave instability can be attributed to the Bernoulli effect, which causes the normal force component acting on the wave crest to move in the opposite direction of gravity. This phenomenon is mainly caused by the pressure difference, which pushed the liquid up to hit the upper surface of the pipe. For a fully developed slug at 81 D, a fast-growing holdup is present, followed by a highly reduced one.

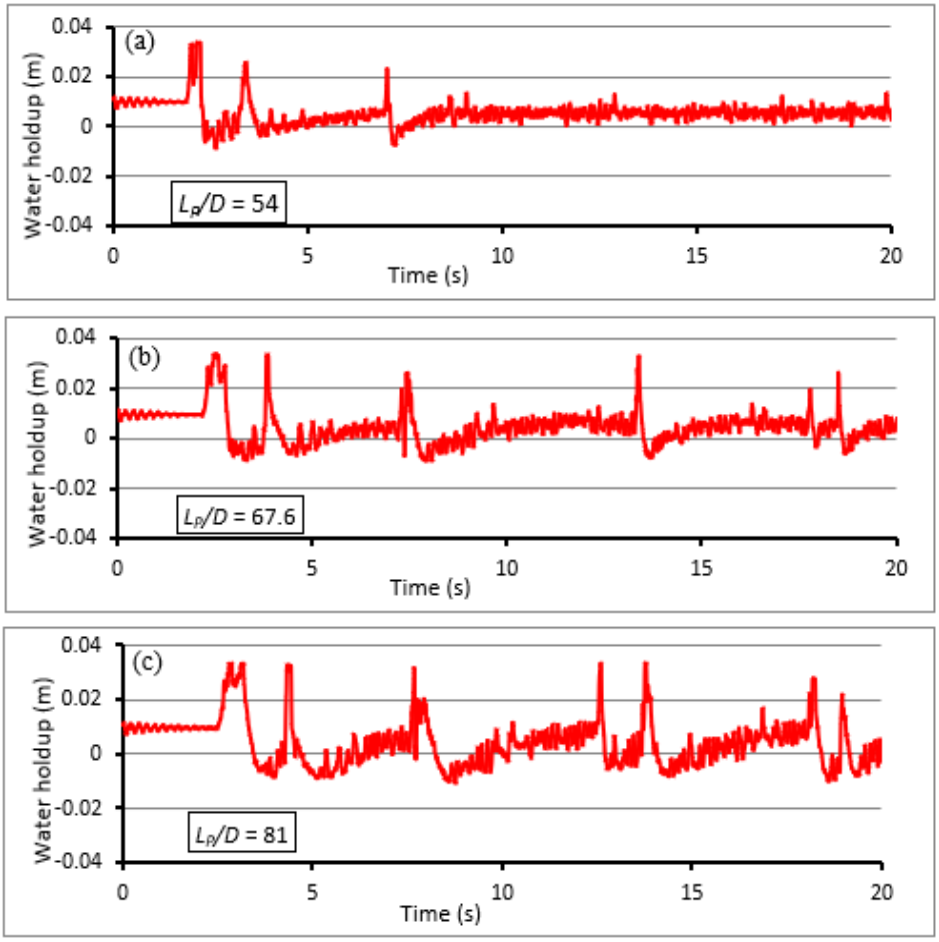


**Fig. 10.** Water slug development under the simulation of Case 3 at three different locations along the pipe: (a) $L_P/D$ = 54; (b) $L_P/D$ = 67; (c) $L_P/D$ = 81

Another phenomenon realised from the simulation is that when the water superficial velocity was increased whilst the air superficial velocity was fixed, the initiation moved away from the inlet. This behaviour implies that the initiation of the slug was delayed. By contrast, when the water superficial velocity was fixed whilst the air superficial velocity was increased, the initiation of the slug occurred near the inlet. In other words, the slug flow is more affected by the liquid phase than the gaseous phase. This result can be attributed to the higher density of the liquid than the gas, which imposes a larger momentum on the flow. This finding is also noted in the monitoring of the slug initiation during the experiments.

### *4.2 Experimental Analysis of the Mean Slug Body Lengths*

Figure 11 displays the observations of the slug body region captured by the high-speed camera as a set of snap shots. The images depict the effect of gas and water superficial velocities on the water slug length. The water slug length was measured by selecting the x-coordinates for the front and rear for each set of inlet flow conditions (Figure 12).

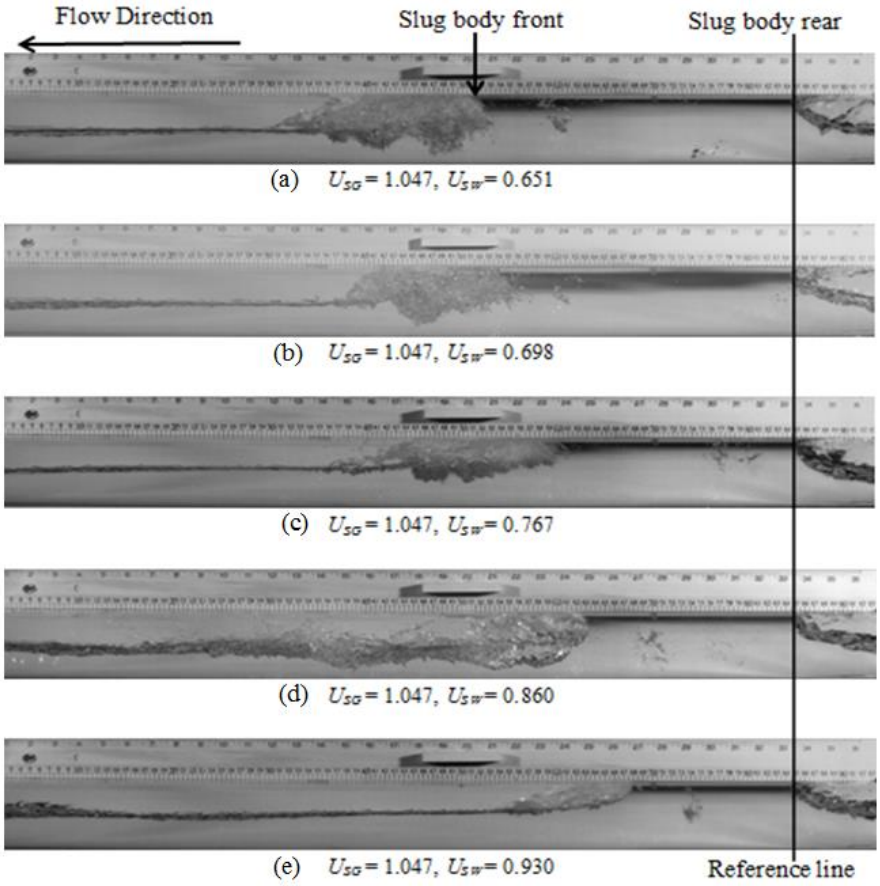


**Fig. 11.** Water slug body lengths at various superficial velocities: (a) $U_{SW}$ = 0.651 m/s; (b) $U_{SW}$ = 0.698 m/s; (c) $U_{SW}$ = 0.767 m/s; (d) $U_{SW}$ = 0.860 m/s; (e) $U_{SW}$ = 0.930 m/s

The reference line was located at 6 m from the inlet. The water slug body length was estimated by subtracting the front from the rear.

$$L_s = X_{front} - X_{rear}$$

The mean slug body length can be calculated as

$$L_S = \frac{1}{N}\sum_{n=1}^{N} L_{s,n}$$

where $N$ is the number of repeated slugs obtained from the measurements for the same flow conditions.

For a given water superficial velocity, Ferré [32] observed that within the range of 0.5 > $U_{SG}$ > 4 m/s, the mean liquid slug length was increasing in a pipe with a length 50 m and a diameter of 45 mm. Woods [33] reported that the mean liquid slug length is slightly increasing within the range of 1.0 > $U_{SG}$ > 3.0 m/s in a pipe with a diameter of 76 mm and a length of 19.8 m.

Figure 12 shows that when the air superficial velocity was increased for a given water superficial velocity, the water slug length increased. These observations are consistent with the trend observed by Kordyban [34] and Ban et al., [35]. The maximum $L_S$/D was equal to 14.73, which was obtained at $U_{SW}$ = 0.651 m/s and $U_{SG}$ = 2.792 m/s.

On the contrary, the water slug length decreased when the water superficial velocity increased. If the water superficial velocity increases at a constant air superficial velocity, then the ratio of the liquid to the gas in the slug unit will also increase. The slug body length will therefore decrease (Figure 12). The minimum $L_S$/D at $L_P$ = 6 m was equal to 3.5, which was obtained at $U_{SW}$ = 0.86 m/s and $U_{SG}$ = 0.698 m/s. Furthermore, the water slug length for all experimental conditions ranged at around 3.5–14.6 D. However, the slug body length increased as the slug travelled along the downstream pipeline.

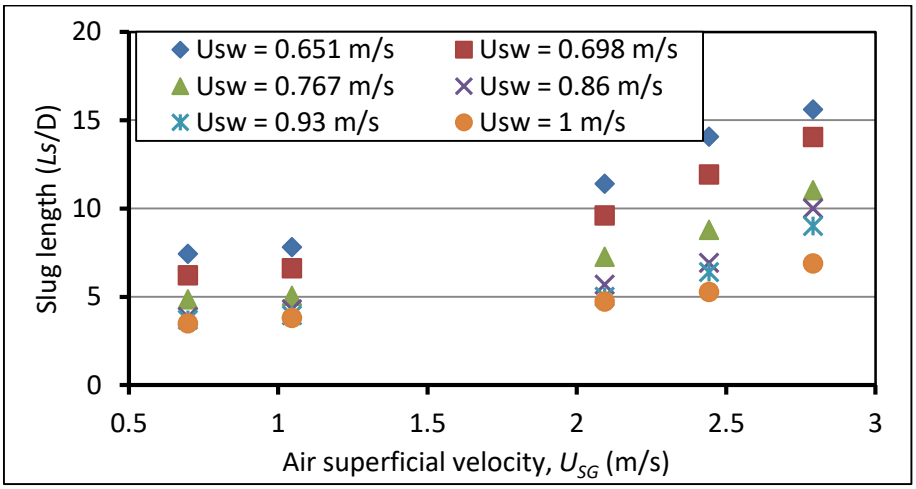


**Fig. 12.** Effect of air and water superficial velocities on the water slug body length at $L_P$ = 6 m

*4.2.1 Experimental analysis of the mean water slug frequencies*

The slug frequency $F_S$ is defined as the reciprocal of the slug unit cross period or the mean number of slugs per unit time as seen by a fixed observer.

$$F_s = \frac{1}{\Delta t} \quad (9)$$

To achieve an accurate estimation of the slug frequency, $F_S$ can be defined as the mean of $N$ number of slugs per unit time as seen by a fixed observer. The mean slug frequency can be obtained as

$$F_s = \frac{1}{N} \sum_{n=1}^{n=N} \frac{1}{\Delta t_n} \quad (10)$$

Figure 13 shows the frequency distribution data of a slug flow monitored in a horizontal pipe 6 m from the fluid inlet zone. For approximately the same superficial velocities, the frequency in Figure 13 was higher than those reported by Woods and Hanratty [12] and Carneiro *et al.,* [14]. However, in the three works, the frequency decreased with the increase in the $U_{SG}$ at a given $U_{SW}$. The minimum frequencies were obtained at the lowest experimented $U_{SW}$ (0.651 m/s). Comparative studies showed that the slug frequencies obtained in the current work by high-speed video footage were in good agreement with those obtained from the analysis of the pressure pulse measurements by Woods and Hanratty [12] and Carneiro *et al.,* [14].

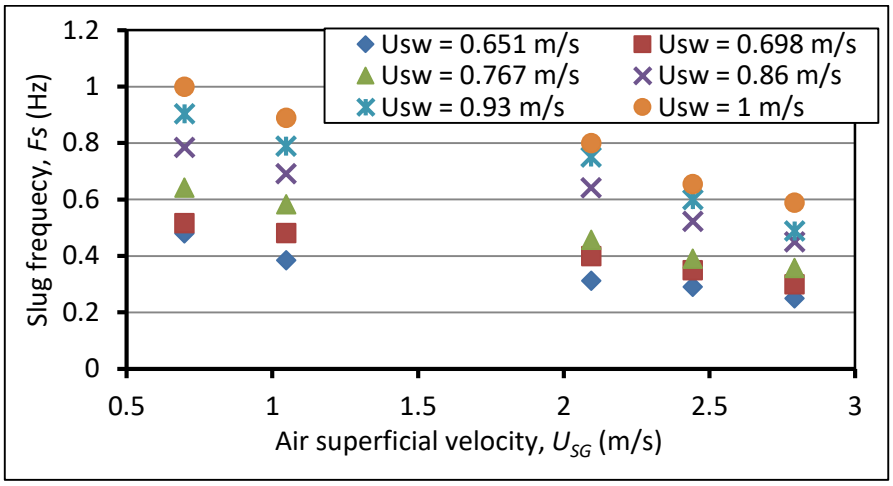


**Fig. 13.** Effect of air and water superficial velocities on the slug frequencies at $L_P$ = 6 m

The experimental results demonstrate that when the water superficial velocity increased, the slug frequency increased, whereas the increase in air superficial velocity decreases the slug frequency. These phenomena suggest that the frequency and water slug length were inversely proportional for the constant water and air superficial velocities (Figure 14 and 15, respectively).

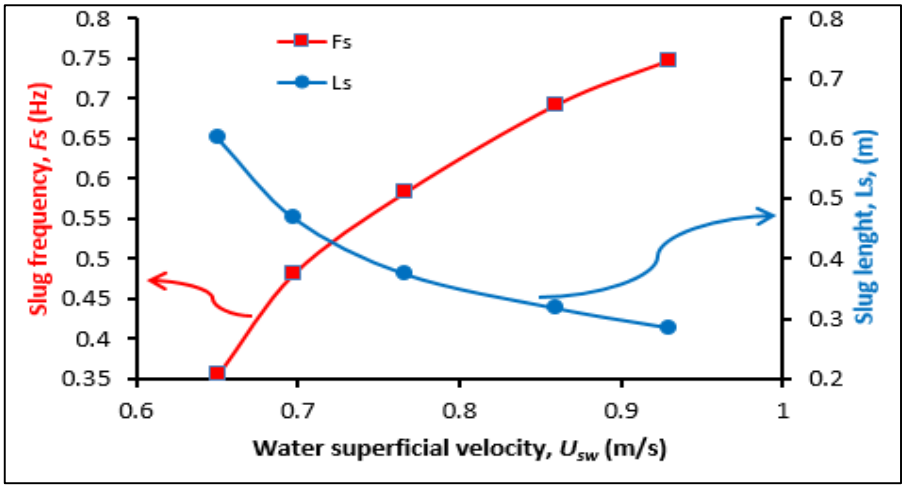


**Fig. 14.** Comportment of water slug length and slug frequency at various water superficial velocities (air superficial velocity = 1.047 m/s)

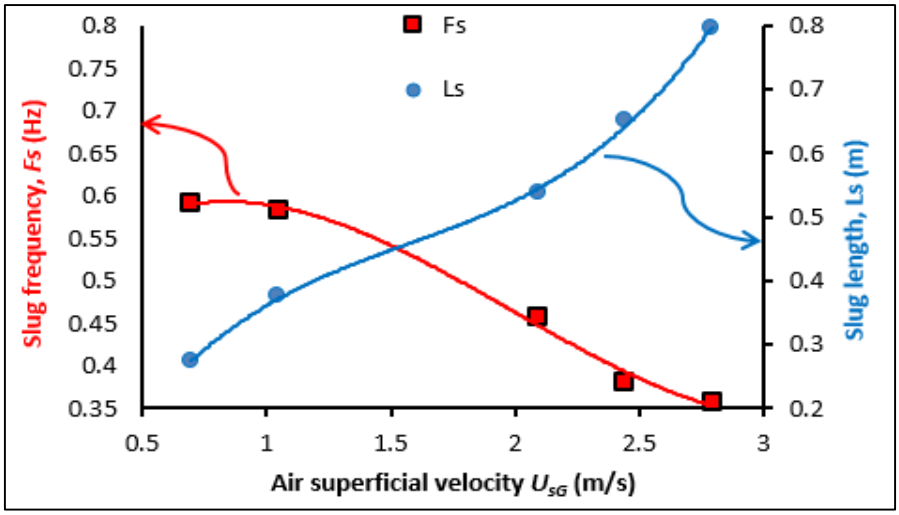


**Fig. 15.** Comportment of water slug length and slug frequency at various air superficial velocities (water superficial velocity = 0.767 m/s)

### *4.3 Numerical versus Experimental Results*

The numerical results are compared with the experimental ones to validate the numerical procedure developed in the present investigation. Six simulation cases were selected: three cases for various water superficial velocities at a fixed air superficial velocity and another three for various air superficial velocities at a fixed water superficial velocity. Table 3 summarises the three cases.

**Table 3**
Simulation cases adopted for the computational analysis

| Case | $U_{SG}$ | $U_{SW}$ |
|---|---|---|
| Case 1 | | 0.651 m/s |
| Case 2 | 2.443 m/s | 0.767 m/s |
| Case 3 | | 1.0 m/s |
| Case 4 | 2.094 m/s | |
| Case 5 | 2.443 m/s | 1.0 m/s |
| Case 6 | 3.141 m/s | |

### 4.3.1 Comparison of mean water slug body lengths

Tables 4 and 5 present the numerical and experimental results of the water slug length, respectively, for fixed air and water superficial velocities of 2.443 and 1.0 m/s.

In Table 4, the slug water lengths in simulation Cases 1, 2 and 3 are higher than that in the experimental tests. The mean difference between the simulation and experiment is 7.028%.

In Table 5, the experimental values of the slug length for Cases 4, 5 and 6 are 4.73, 6.21 and 7.97 times the pipe diameter, respectively, whereas the slug lengths predicted by the simulation are 4.98, 5.27 and 8.96 times the pipe diameter, respectively. A maximum difference of 15.1% is observed at Case 5, whereas the average difference between the simulation and experiment for the water slug length is 10.38%.

**Table 4**
Experimental and simulation results of the mean water slug length at $U_{SG}$ = 2.443 m/s

| Simulation cases with ($U_{SW}$) | Exp. ($L_s/D$) | Numerical ($L_s/D$) | % difference |
|---|---|---|---|
| Case 1 0.651 m/s | 14.459 | 14.555 | 0.658 |
| Case 2 0.767 m/s | 8.784 | 9.276 | 5.304 |
| Case 3 1.0 m/s. | 5.270 | 6.209 | 15.123 |
| Mean percentage of difference | | | 7.028 |

**Table 5**
Experimental and simulation results of the mean water slug length at $U_{SW}$ = 1.0 m/s

| Simulation cases with ($U_{SG}$) | Exp. ($L_s/D$) | Numerical ($L_s/D$) | % difference |
|---|---|---|---|
| Case 4: 2.094 m/s | 4.730 | 4.980 | 5.020 |
| Case 5: 2.443 m/s | 5.270 | 6.210 | 15.120 |
| Case 6: 3.141 m/s | 7.970 | 8.960 | 10.980 |
| Mean percentage of difference | | | 10.380 |

Ban *et al.,* simulated various two-phase flow regimes on a 0.08-m-diameter horizontal pipe through CFD and FLUENT 16.1. They adopted the current experimental results and reported that the simulation results of slug body length are in good agreement with the experimental data. They gained a similar inference, in which a high ratio of gas to liquid leads to a large mixing zone for the same slug unit length.

### 4.3.2 Comparison of slug frequency

The numerical slug frequency phenomenon exhibited a similar behaviour as that in the experiments. Tables 6 and 7 present the investigation of the effect of increasing the air and water superficial velocities on the mean slug frequencies, respectively. When the air superficial velocity was

a fixed at 2.443 m/s and the water superficial velocities were set to 0.651, 0.776 and 1.0 m/s, the measured and numerically predicted slug frequencies varied within a range of −9.848%, 12.844% and 1.355%, respectively. The differences were inconsistent; at 0.651 m/s, the experimentally measured slug frequency was higher than the predicted one, whereas at 0.767 and 1.0 m/s, the numerically predicted slug frequency was higher than the measured one. The numerical slug frequencies agreed with the experimental results. At a constant air superficial velocity and varying water superficial velocities, the mean difference in the slug frequencies between the simulation and experimental results was within 1.450%.

**Table 6**
Experimental and simulation results of the mean slug frequencies at constant $U_{SG}$ and varying $U_{sw}$ (m/s)

| $U_{sw}$ (m/s) | $U_{sg}$ (m/s) | Experimental slug frequency (Hz) | Numerical slug frequency (Hz) | % difference |
|---|---|---|---|---|
| 0.651 | | 0.290 | 0.264 | −9.848 |
| 0.767 | 2.443 | 0.380 | 0.436 | 12.844 |
| 1.0 | | 0.655 | 0.664 | 1.355 |
| Mean percentage of difference | | | | 1.450 |

Table 7 shows the comparison of the slug frequencies from the experimental and simulation predictions with respect to the air superficial velocities. At air superficial velocities of 2.094 and 2.443 m/s, the simulated slug frequency was higher than the experimental one, whereas at 3.141 m/s, the numerically predicted frequency was less than the measured value. The maximum difference between the simulation and experimental slug frequencies at a constant water superficial velocity was 1.355%, and the mean over the entire range of air superficial velocities was 0.374%.

**Table 7**
Experimental and simulation results of the mean slug frequencies at constant $U_{SW}$ and varying $U_{sg}$ (m/s)

| $U_{sg}$ (m/s) | $U_{sw}$ (m/s) | Experimental slug frequency (Hz) | Numerical slug frequency (Hz) | % difference |
|---|---|---|---|---|
| 2.094 | | 0.829 | 0.832 | 0.361 |
| 2.443 | 1.0 | 0.655 | 0.664 | 1.355 |
| 3.141 | | 0.509 | 0.506 | −0.593 |
| Mean percentage of difference | | | | 0.374 |

## 5. Conclusions

This study conducted an experimental investigation on air/water slug flow in a horizontal transparent pipe with a diameter of 0.074 m and length of 8.0 m. A numerical procedure, which utilised the STAR-CCM+ software, successfully simulated and captured the slug flow pattern, slug initiation and slug growth. The VOF model demonstrated a vast capability in capturing the interface between the air and water phases with reasonable likeness to that of the experimental interface. The following conclusions are drawn.

i. The CFD simulations of the slug body length, slug frequency and slug initiation and the development demonstrate an acceptable agreement with the experimental measurements.
ii. The slug initiation is strongly dependent on the water and air superficial velocities. At a fixed air superficial velocity, when the water superficial velocity is increased, the slug initiation

position moves farther downstream from the inlet. Conversely, when the water superficial velocity is fixed and the air superficial velocity is increased, the slug initiation position moves near the inlet.

iii. The mean water slug length obtained from various investigated fluids' superficial velocities ranges within 3.5–15 times the pipe diameter. The slug length decreases with the increase in water superficial velocity and increases with the increase in air superficial velocity.

iv. The liquid phase greatly influences the slug frequency reduction. The slug frequency decreases by approximately 0.25 $s^{-1}$ when the air superficial velocity increases by 50% and increases by around 1.88 $s^{-1}$ when the water superficial velocity increases by 50%.

v. The time traces of the water holdup indicate that slugs are formed as a result of the local instability at the wave crest rather than due to the instability of the entire wave.

In the future, the fluid structure interaction by slug in pipe flow should be investigated, and the effects of the gas and water superficial velocities on the induced vibration behaviour should be identified.

**Acknowledgement**
The authors of this work express their profound gratitude to the Universiti Teknologi PETRONAS for supporting the research work technically and logistically. Ministry of Higher Education (MOHE) – Malaysia is acknowledged for providing the financial support under research grant FRGS/1/2017/STG02/UTP/01/1 [CS: 0153AB-L58]. The second author acknowledges Universiti Teknologi PETRONAS for supporting his PhD under the Graduate Assistance scheme (GA). Also, acknowledges are due to the Iraqi government – Ministry of Oil for providing the study leave for the second author.

**References**

[1] Sharma, Y., M. Ihara, and R. Manabe. "Simulating slug flow in Hilly-Terrain pipelines." In *SPE International Petroleum Conference and Exhibition in Mexico*. Society of Petroleum Engineers, 2002.

[2] Godhavn, John-Morten, Mehrdad P. Fard, and Per H. Fuchs. "New slug control strategies, tuning rules and experimental results." *Journal of Process Control* 15, no. 5 (2005): 547-557.

[3] Issa, R. I., and M. H. W. Kempf. "Simulation of slug flow in horizontal and nearly horizontal pipes with the two-fluid model." *International Journal of Multiphase Flow* 29, no. 1 (2003): 69-95.

[4] Sanchis, Arnaud, George W. Johnson, and Atle Jensen. "The formation of hydrodynamic slugs by the interaction of waves in gas–liquid two-phase pipe flow." *International Journal of Multiphase Flow* 37, no. 4 (2011): 358-368.

[5] Sharma, S., S. Lewis, and G. Kojasoy. "Local studies in horizontal gas–liquid slug flow." *Nuclear Engineering and Design* 184, no. 2-3 (1998): 305-318.

[6] Dukler, Abraham E., and Martin G. Hubbard. "A model for gas-liquid slug flow in horizontal and near horizontal tubes." *Industrial & Engineering Chemistry Fundamentals* 14, no. 4 (1975): 337-347.

[7] Nicholson, M. K. "K., Aziz, and GA Gregory. "Intermittent two phase flow in horizontal pipes: Predictive Models." *Can. J. Chem. Eng* 56 (1978): 653-663.

[8] Gregory, G. A., M. K. Nicholson, and K. Aziz. "Correlation of the liquid volume fraction in the slug for horizontal gas-liquid slug flow." *International Journal of Multiphase Flow* 4, no. 1 (1978): 33-39.

[9] Scott, Stuart L., Ovadia Shoham, and James P. Brill. "Prediction of slug length in horizontal, large-diameter pipes." *SPE Production Engineering* 4, no. 3 (1989): 335-340.

[10] Nydal, O. J., Sandro Pintus, and Paolo Andreussi. "Statistical characterization of slug flow in horizontal pipes." *International Journal of Multiphase Flow* 18, no. 3 (1992): 439-453.

[11] Fan, Z., F. Lusseyran, and T. J. Hanratty. "Initiation of slugs in horizontal gas-liquid flows." *AIChE Journal* 39, no. 11 (1993): 1741-1753.

[12] Woods, Bennett D., and Thomas J. Hanratty. "Influence of Froude number on physical processes determining frequency of slugging in horizontal gas–liquid flows." *International Journal of Multiphase Flow* 25, no. 6-7 (1999): 1195-1223.

[13] Mohmmed, Abdalellah O., Hussain H. Al-Kayiem, Mohammad S. Nasif, and Rune W. Time. "Effect of slug flow frequency on the mechanical stress behavior of pipelines." *International Journal of Pressure Vessels and Piping* 172 (2019): 1-9.
[14] Carneiro, J. N. E., R. Fonseca Jr, A. J. Ortega, R. C. Chucuya, A. O. Nieckele, and L. F. A. Azevedo. "Statistical characterization of two-phase slug flow in a horizontal pipe." *Journal of the Brazilian Society of Mechanical Sciences and Engineering* 33, no. SPE1 (2011): 251-258.
[15] Al-Kayiem, Hussain H., Abdalellah O. Mohmmed, Zahid I. Al-Hashimy, and Rune W. Time. "Statistical assessment of experimental observation on the slug body length and slug translational velocity in a horizontal pipe." *International Journal of Heat and Mass Transfer* 105 (2017): 252-260.
[16] López, Jorge, Hugo Pineda, David Bello, and Nicolás Ratkovich. "Study of liquid–gas two-phase flow in horizontal pipes using high speed filming and computational fluid dynamics." *Experimental Thermal and Fluid Science* 76 (2016): 126-134.
[17] Pineda-Pérez, H., T. Kim, E. Pereyra, and N. Ratkovich. "CFD modeling of air and highly viscous liquid two-phase slug flow in horizontal pipes." *Chemical Engineering Research and Design* 136 (2018): 638-653.
[18] Mohmmed, Abdalellah O., Mohammad S. Nasif, Hussain H. Al-Kayiem, and Rune W. Time. "Measurements of translational slug velocity and slug length using an image processing technique." *Flow Measurement and Instrumentation* 50 (2016): 112-120.
[19] Mohmmed, A. O. I. "Effect of Slug Two-Phase Flow on Fatigue of Pipe Material." (2016).
[20] IAEA, TECDOC. "1585 Measurement uncertainty: A practical guide for secondary standards dosimetry laboratories." *IAEA, Vienna* (2008).
[21] Pinilla, Jorge Andres, Esteban Guerrero, Hugo Pineda, Raquel Posada, Eduardo Pereyra, and Nicolas Ratkovich. "CFD modeling and validation for two-phase medium viscosity oil-air flow in horizontal pipes." *Chemical Engineering Communications* 206, no. 5 (2019): 654-671.
[22] Rashimi, W., T. S. Y. Choong, T. G. Chuah, S. A. Hussain, and M. Khalid. "Effect of interphase forces on two phase liquid: liquid flow in horizontal pipe." *Inst Eng* 71 (2010): 35-40.
[23] Frank, Thomas. "Numerical simulation of slug flow regime for an air-water two-phase flow in horizontal pipes." In *Proceedings of the 11th International Topical Meeting on Nuclear Reactor Thermal-Hydraulics (NURETH-11), Avignon, France, October*, pp. 2-6. 2005.
[24] Khalid Al-Jassim. "Numerical simulations of stratified two and three phase turbulent flows in pipelines." PhD thesis, University of Basrah, Iraq, 2009.
[25] Iacovides, H., G. Kelemenis, and M. Raisee. "Flow and heat transfer in straight cooling passages with inclined ribs on opposite walls: an experimental and computational study." *Experimental Thermal and Fluid Science* 27, no. 3 (2003): 283-294.
[26] Menter, Florian R. "Two-equation eddy-viscosity turbulence models for engineering applications." *AIAA Journal* 32, no. 8 (1994): 1598-1605.
[27] Yang, Yi, Ming Gu, and Xinyang Jin. "New inflow boundary conditions for modeling the neutral equilibrium atmospheric boundary layer in SST k-ω model." *J. Wind Eng. Ind. Aerod* (2012).
[28] Wilcox, David C. *Turbulence modeling for CFD*. Vol. 2. La Canada, CA: DCW industries, 1998.
[29] Al-Hashimy, Z. I., H. H. Al-Kayiem, Z. K. Kadhim, and A. O. Mohmmed. "Numerical simulation and pressure drop prediction of slug flow in oil/gas pipelines." *Computational Methods in Multiphase Flow* 8, no. 89 (2015): 57.
[30] Aagaard, Olav. "Hydroelastic analysis of flexible wedges." Master's thesis, Institutt for Marin Teknikk, 2013.
[31] Chica, Leonardo. "FSI study of internal multiphase flow in subsea piping components." MSc thesis, University of Houston, 2014.
[32] Ferré, Daniel. "Écoulements diphasiques à poches en conduite horizontale." *La Houille Blanche* 6-7 (1979): 378-381.
[33] Woods, Bennett David. "Slug formation and frequency of slugging in gas-liquid flows." PhD thesis, University of Illinois at Urbana-Champaign, 1998.
[34] Kordyban, Eugene. "Some details of developing slugs in horizontal two-phase flow." *AIChE Journal* 31, no. 5 (1985): 802-806.
[35] Ban, Sam, William Pao, and Mohammad Shakir Nasif. "Numerical simulation of two-phase flow regime in horizontal pipeline and its validation." *International Journal of Numerical Methods for Heat & Fluid Flow* 28, no. 6 (2018): 1279-1314.